

# Nuclear multifragmentation time-scale and fluctuations of largest fragment size

D. Gruyer,<sup>1</sup> J.D. Frankland,<sup>1,\*</sup> R. Botet,<sup>2</sup> M. Płoszajczak,<sup>1</sup> E. Bonnet,<sup>1</sup> A. Chbihi,<sup>1</sup> G. Ademard,<sup>3</sup>  
 M. Boisjoli,<sup>1,4</sup> B. Borderie,<sup>3</sup> R. Bougault,<sup>5</sup> D. Guinet,<sup>6</sup> P. Lantesse,<sup>6</sup> L. Manduci,<sup>7</sup> N. Le Neindre,<sup>5</sup>  
 P. Marini,<sup>1</sup> P. Pawłowski,<sup>8</sup> M. F. Rivet,<sup>3</sup> E. Rosato,<sup>9</sup> G. Spadaccini,<sup>9</sup> M. Vigilante,<sup>9</sup> and J.P. Wieleczko<sup>1</sup>

(INDRA collaboration)

<sup>1</sup>*GANIL, CEA-DSM/CNRS-IN2P3, Bvd. Henri Becquerel, F-14076 Caen CEDEX, France*

<sup>2</sup>*Laboratoire de Physique des Solides, CNRS UMR8502,*

*Université de Paris-Sud bât. 510, F-91405 Orsay CEDEX, France*

<sup>3</sup>*Institut de Physique Nucléaire, CNRS/IN2P3, Université Paris-Sud 11, F-91406 Orsay CEDEX, France*

<sup>4</sup>*Département de physique, de génie physique et d'optique, Université Laval, Québec, G1V 0A6 Canada*

<sup>5</sup>*LPC, CNRS/IN2P3, Ensicaen, Université de Caen, F-14050 Caen CEDEX, France*

<sup>6</sup>*Institut de Physique Nucléaire, Université Claude Bernard Lyon 1,*

*CNRS/IN2P3, F-69622 Villeurbanne CEDEX, France*

<sup>7</sup>*École des Applications Militaires de l'Énergie Atomique, B.P. 19, F-50115 Cherbourg, France*

<sup>8</sup>*H. Niewodniczański Institute of Nuclear Physics, PL-31342 Kraków, Poland*

<sup>9</sup>*Dipartimento di Scienze Fisiche e Sezione INFN,*

*Università di Napoli "Federico II," I-80126 Napoli, Italy*

We show that the biggest fragment charge distribution in central collisions of  $^{129}\text{Xe}+^{nat}\text{Sn}$  leading to multifragmentation is an admixture of two asymptotic distributions observed for the lowest and highest bombarding energies. The evolution of the relative weights of the two components with bombarding energy is shown to be analogous to that observed as a function of time for the largest cluster produced in irreversible fragmentation for a finite system. This analogy allows us to speak of pseudo-critical nuclear multifragmentation around  $E_{beam} \approx 30$  MeV/A. We infer that the size distribution of the largest fragment in nuclear multifragmentation is also characteristic of the time scale of the process, which is largely determined by the onset of radial expansion in this energy range.

PACS numbers: 25.70.Pq

Phase transitions occupy a central place in many fields of physics such as condensed matter, collisions of atomic aggregates, and most recently, in formation of quark-gluon plasma in ultra-relativistic hadron collisions. They allow to investigate the equation of state and phase diagram of the system under study. The case of nuclear multifragmentation, as observed in intermediate energy heavy-ion collisions [1], provides a unique opportunity to study not only thermodynamical properties of nuclear matter, but also phase transitions in *finite* systems.

The universal character of order parameter fluctuations in finite systems [2, 3], provides a good framework in which to address such questions. Using such a model-independent analysis, it was shown that the size (atomic number) of the largest fragment produced in multifragmentation events,  $Z_{max}$ , behaves like an order parameter, *i.e.* the scaling properties of its fluctuations change with increasing energy [4]. In this sense nuclear multifragmentation belongs to a large class of phase transitions or critical phenomena for which the size of the largest cluster is the order parameter, for example site- or bond-percolation on lattices, reversible or irreversible aggregation [2]. Using the latter class of model we will show that we can extend this analogy, by studying the evolution of the order parameter distribution in the critical region.

In [5] it was shown that a distinct asymptotic form of the largest fragment distribution in multifragmentation

can be associated with each scaling regime : a quasi-Gaussian symmetric  $Z_{max}$  distribution at low bombarding energies, and an asymmetric Gumbel distribution [6] in the high-energy disordered regime. In this letter we will study in more detail the transition from one regime to the other, using new data on  $Z_{max}$  distributions for  $^{129}\text{Xe}+^{nat}\text{Sn}$  central collisions measured with INDRA [7] at bombarding energies intermediate between the two asymptotic regimes. We will show that, in fact, the  $Z_{max}$  distributions evolve continuously from one asymptotic distribution to the other with increasing bombarding energy, and, by analogy with the evolution of the order parameter distribution in the irreversible aggregation model, deduce a link between  $Z_{max}$  fluctuations and the time-scale of nuclear multifragmentation.

The irreversible aggregation model describes an out-of-equilibrium clusterization process, whose order parameter is the average size of the largest cluster at any given time,  $s_{max}$ . The evolution of the droplet size population is given by the Smoluchowski equations [8],

$$\frac{dc_s}{dt} = \frac{1}{2} \sum_{i+j=s} K_{ij} c_i c_j - \sum_{i=1}^N K_{is} c_i c_s \quad (1)$$

where  $c_s$  is the concentration of droplets of size  $s$ ,  $K_{\alpha\beta}$  is the coalescence probability per unit of time between two droplets of respective size  $\alpha$  and  $\beta$ ,  $K_0$  is a

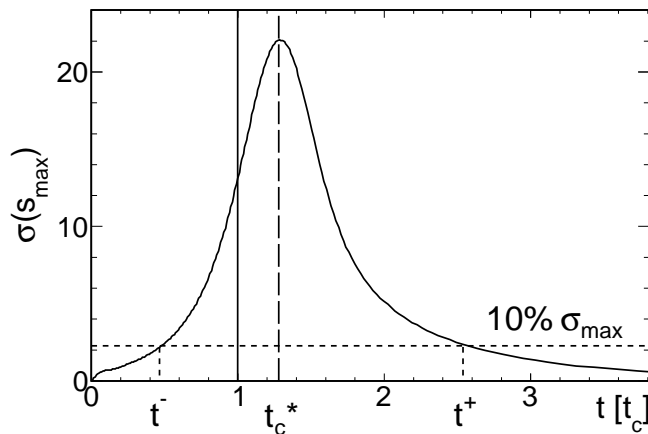


Figure 1: Standard deviation of the largest cluster size,  $\sigma(s_{\max})$ , as a function of the time  $t$ , for irreversible aggregation with  $N = 216$ ;  $t_c^*$ ,  $t^-$  and  $t^+$  are the pseudo-critical time and the limits of the critical domain (see text).

constant and  $N$  is the size of the system. This model exhibits a second-order phase transition after a critical time,  $t_c$  [8].

Precise limits of the critical domain for finite systems, where the correlation length becomes comparable to the size of the system [9], are not easily obtained. An estimation using the width of the largest cluster size distribution,  $\sigma(s_{\max})$ , has been proposed in [10]. In the infinite system, this critical quantity must diverge at the critical time. As shown in Fig. 1, for a finite system with  $N = 216$  particles,  $\sigma(s_{\max})$  reaches a sharp maximum at the pseudo-critical time,  $t_c^* = 1.28t_c$ . We define the lower and upper limits of the critical domain,  $t^-$  and  $t^+$ , as the times at which  $\sigma(s_{\max})$  is above 10% of its maximum:  $t^- = 0.5t_c$  and  $t^+ = 2.6t_c$  (see Fig. 1).

The order parameter distribution for irreversible aggregation is not known exactly, but it was proposed that the asymptotic  $s_{\max}$  distribution for  $t \ll t_c^*$  is that of Gumbel [10]. The average size of the largest cluster evolves with time as more and more coalescence of smaller clusters takes place. At long times, the order parameter is then essentially of additive nature. From the central limit theorem, this results in an asymptotic Gaussian distribution of  $s_{\max}$  for  $t \gg t_c^*$ . In the critical domain, for  $t^- < t < t^+$ , fluctuations are so large that similarly prepared systems can exhibit one or the other behavior. This suggests that the effective  $s_{\max}$  distribution for an ensemble of systems, at any given intermediate time, is an admixture of a Gaussian distribution and a Gumbel distribution.

We performed numerical simulations of the Smoluchowski equations, Eq.(1), for finite systems with  $N \sim 50 - 200$  particles, comparable with nuclear system sizes. The obtained  $s_{\max}$  distributions were then fitted with the following admixture of Gaussian and Gumbel distri-

butions:

$$f(x) = \eta f_{Ga}(x) + (1 - \eta) f_{Gu}(x), \quad (2)$$

where,

$$f_{Ga}(x) = \frac{1}{\sigma\sqrt{2\pi}} \exp\left(-\frac{(x - \mu)^2}{2\sigma^2}\right),$$

$$f_{Gu}(x) = \frac{1}{b_m} \exp\left[-\frac{(x - a_m)}{b_m} - \exp\left(-\frac{(x - a_m)}{b_m}\right)\right],$$

and  $x = s_{\max}$ . The five parameters ( $\eta$ ,  $\mu$ ,  $\sigma$ ,  $a_m$  and  $b_m$ ) are left to vary freely, apart from the constraint that  $\eta$  should be between zero and one. Fits were performed using a binned maximum-likelihood estimation method [11]. In order to quantify the evolution of the relative weight of each distribution, we introduce the ratio:

$$R = \frac{I_{Ga} - I_{Gu}}{I_{Ga} + I_{Gu}} = 2\eta - 1 \quad (3)$$

where  $I_{Ga}$  and  $I_{Gu}$  are the integral of the components defined in Eq.(2). This ratio equals +1 for a pure Gaussian distribution and -1 for a pure Gumbel distribution.

The results of the fitting procedure applied to the distribution of the largest cluster size between  $t^-$  and  $t^+$  are presented in Fig. 2. At short times,  $t^- < t < t_c^*$ , the distribution is almost purely ‘‘Gumbellian’’, with a small Gaussian component (Fig. 2(a)), and the ratio  $R \approx -1$  (Fig. 2(e)). As time increases, the Gaussian component increases, such that between the infinite-system critical time  $t_c$  (Fig. 2(b)) and the pseudo-critical time  $t_c^*$  (Fig. 2(c)), both components have comparable weights, and the ratio  $R$  passes through zero (Fig. 2(e)). The very large fluctuations of  $s_{\max}$  observed at these times in Fig.1 are due to the superposition of the two distributions, whose combined width is far greater than the intrinsic variance of each component. Finally, for the longest time-scales, the Gumbel component disappears (Fig. 2(d)) and  $R$  tends towards +1 (Fig. 2(e)).

The analysis of Smoluchowski calculations shows that the decomposition of the  $s_{\max}$  distributions into an admixture of two asymptotic distributions seems to be relevant. Similar results were obtained for all simulated system sizes,  $N$ : as  $N$  increases the transition becomes more abrupt and the value  $R = 0$  occurs closer and closer to  $t_c$ . It should be noted that we have obtained similar results with a three-dimensional percolation model [12], which describes the at-equilibrium formation of clusters on a geometric lattice as a function of bond probability,  $p$ , with a second-order transition at the critical probability,  $p_c$ . Such models have often been used to study criticality in nuclear multifragmentation [13, 14]. In all cases the value  $R = 0$  occurs in the critical region of the underlying phase transition, between the infinite-system critical point and the  $N$ -dependent maximum of  $s_{\max}$  fluctuations. We will now apply the same analysis to

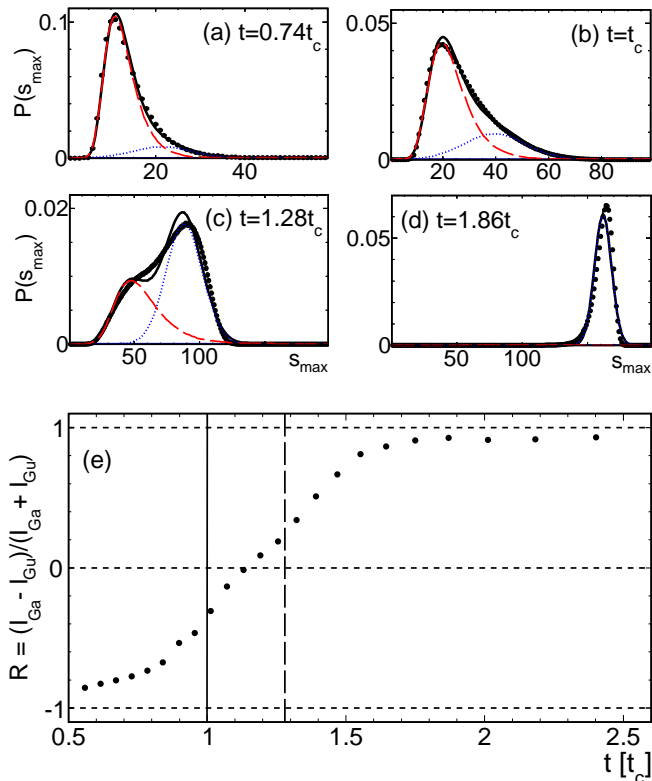


Figure 2: (color online) Analysis of Smoluchowski calculations for  $N = 216$  particles: (a-d) distribution of the size of the largest cluster  $P(s_{\max}) = (1/N)dN/ds_{\max}$  for different times in the critical domain; (Black solid curve) best fit to the data using Eq.(2); (Red dashed curve) Gumbel component; (Blue dotted curve) Gaussian component; (e) evolution of the ratio  $R$  between the two components (Eq.(3)) in the critical domain (see Fig. 1), as a function of the time  $t$  in unit of  $t_c$  (see text); vertical lines are the same as in Fig. 1.

the largest fragment distributions measured for nuclear multifragmentation in central heavy-ion collisions.

Collisions of  $^{129}\text{Xe} + ^{nat}\text{Sn}$  were measured using the IN-DRA  $4\pi$  array at the GANIL accelerator facility. This charged product detector, composed of 336 detection cells arranged according to 17 rings centered on the beam axis, covers 90% of the solid angle. More experimental details can be found in [5, 7, 15]. Data were taken during two separate campaigns. Beam energies of 27, 29, and 35 MeV/A have been performed specifically in order to probe in more detail the energy range around the change of scaling regime observed in [4]: those data are presented here for the first time.

As in previous works [4, 5], we study multifragmentation events occurring in central collisions, requiring the geometrical overlap between projectile and target to be as close as possible to total. In addition, the correct measurement of the largest fragment distribution requires the detection of nearly all fragments event by event. For this purpose we will use two global variables,  $Et_{12}$  and  $Z_{\text{tot}}$ .

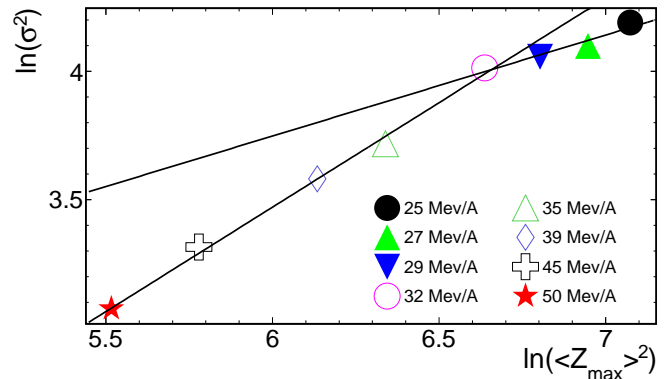


Figure 3: (color online) (Points) Log-log correlation between the first two cumulant moments ( $\langle Z_{\max} \rangle^2$  and  $\sigma^2$ ) of the order parameter's distribution; (Lines) linear fits performed in the range 50-32 MeV/A (resp. 32-25 MeV/A) which correspond to a slope  $\Delta \sim 1$  (resp.  $\Delta \sim 0.5$ ) (see text).

$Et_{12}$  is the total transverse energy of light charged particles ( $Z = 1, 2$ ), which increases with collision centrality [16], while  $Z_{\text{tot}}$  is the sum of the atomic numbers of all detected charged products in each event. In [5] separate energy-dependent cuts were made in the  $Et_{12}$  and  $Z_{\text{tot}}$  distributions. In this new analysis, in order to ensure equivalent selections for all beam energies we retain events which maximize the quantity  $(Et_{12} \times Z_{\text{tot}})$ . For each beam energy, a cut was defined corresponding to the last percentile of the  $(Et_{12} \times Z_{\text{tot}})$  distribution measured with the online trigger condition (charged product multiplicity  $M \geq 4$ ).

Let us first examine the scaling properties of  $Z_{\max}$  fluctuations including the three new data points at 27, 29 and 35 MeV/A. Figure 3 shows the correlations between the first two cumulant moments of the  $Z_{\max}$  distribution ( $\langle Z_{\max} \rangle^2$  and  $\sigma^2$ ), for each beam energy. As in Fig. 1(c) of [4], the data fall on two branches,  $\sigma^2 \sim \langle Z_{\max} \rangle^{2\Delta}$ , with different values for the scaling parameter,  $\Delta$  [2, 3]:  $\Delta \sim 1$  above 32 MeV/A, and  $\Delta \sim 1/2$  below 32 MeV/A. The new data points present a consistent behavior which follows the systematic scaling trend. It should also be noted that the scaling properties of  $Z_{\max}$  distributions in central collisions are quite independent of the detailed selection procedure, as different methods were used to select events in [4, 5].

The results of the fits performed on the  $Z_{\max}$  distribution using Eq.(2) are shown in Fig.4. It can be seen that, for all analyzed energies, a good fit to the experimental distribution is achieved: reduced  $\chi^2$  values all lie between approximately 4 and 10, and can further be reduced if  $Z_{\max}$  distributions are smoothed to remove odd-even staggering of the yields [17]: in that case all  $\chi^2$  values are close to 2, except for data at 32 MeV/A for which a significantly larger value ( $\chi^2 \sim 4$ ) is obtained. At the highest energy considered here (50 MeV/A), the result of the fit is an almost pure Gumbel distribution

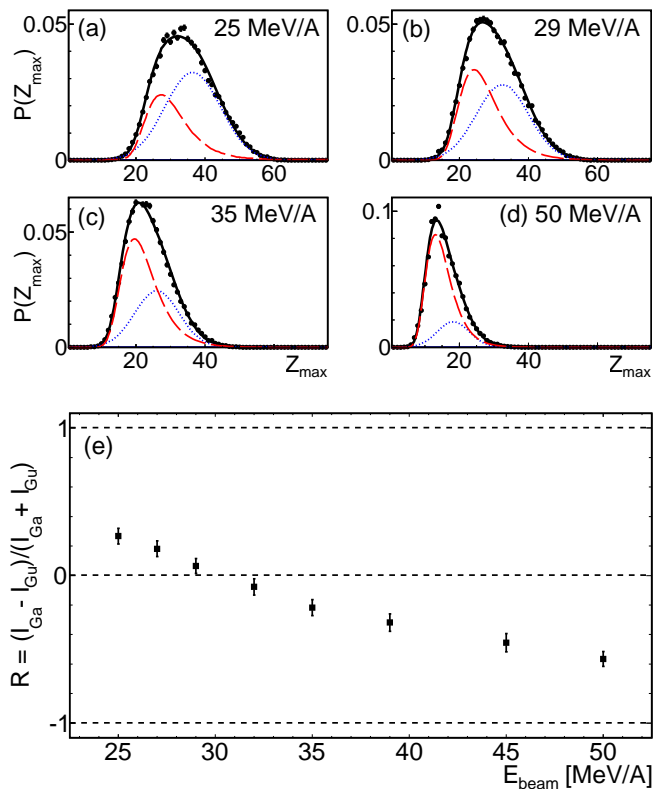


Figure 4: (color online) Analysis of  $^{129}\text{Xe}+^{nat}\text{Sn}$  reactions: (a-d) distribution of the charge of the largest detected fragment  $P(Z_{\max}) = (1/N)dN/dZ_{\max}$  for different beam energies, (Black solid curve) best fit to the data using Eq.(2), (Red dashed curve) Gumbel component, (Blue dotted curve) Gaussian component; and (e) evolution of the ratio  $R$  between the two components (Eq.(3)), as a function of the beam energy.

(Fig. 4(d)). For the other bombarding energies, both contributions are present, and the relative importance of the Gaussian component increases with decreasing energy. The quantity  $R$ , defined in Eq.(3), is evaluated for each bombarding energy, and its evolution is presented in Fig. 4(e). The vertical bars show the uncertainty coming from the fitting procedure:  $\sigma_R = 2\sigma_\eta$ , calculated from Eq.(3). The value  $R = 0$  is reached between 29 and 32 MeV/A, in the same bombarding energy range as the change of  $\Delta$ -scaling (Fig. 3).

A strong similarity can be seen between the results of the analysis for irreversible aggregation (Fig. 2) and central collisions of  $^{129}\text{Xe}+^{nat}\text{Sn}$  (Fig. 4). In the aggregation model the order parameter distribution depends on the length of time during which clusters can form. In central heavy-ion collisions, a determining factor for the time-scale of fragment formation is the radial expansion of the multifragmenting system, which increases with bombarding energy [1]. Fragment sizes can evolve as long as exchanges of nucleons can take place between them, *i.e.* until freeze-out at which the short-range nuclear interaction between fragments ceases and they be-

gin to move apart. It has been shown that for central  $^{129}\text{Xe}+^{nat}\text{Sn}$  reactions the onset of significant radial expansion occurs for beam energies above 25 MeV/A[15]. The similarity between Figs. 2 and 4 can therefore be understood in terms of fragment size distributions being determined on shorter and shorter time-scales due to increasingly rapid expansion.

We can use this interpretation to understand the systematic evolution of  $\Delta$ -scaling with beam energy and system mass presented in [5]: for  $^{58}\text{Ni}+^{58}\text{Ni}$  collisions, measured from 32 MeV/A to 90 MeV/A, a change of  $\Delta$ -scaling and of the form of the  $Z_{\max}$  distribution were observed, as for  $^{129}\text{Xe}+^{nat}\text{Sn}$  but at a higher bombarding energy of 52 MeV/A; for the lighter system  $^{36}\text{Ar}+^{36}\text{KCl}$ , studied from 32 MeV/A to 74 MeV/A, only the  $\Delta = 1/2$  regime was observed, with quasi-Gaussian  $Z_{\max}$  distributions; on the other hand, for the much heavier  $^{197}\text{Au}+^{197}\text{Au}$  system, at bombarding energies between 40 MeV/A and 80 MeV/A, only the  $\Delta = 1$  regime occurs, with Gumbel  $Z_{\max}$  distributions.

Radial expansion in central heavy-ion collisions occurs after significant compression of the incoming nuclear fluid, and as such depends not only on static nuclear matter properties such as incompressibility, but also on transport properties such as the degree of stopping achieved in the collision. The latter increases with the mass of the colliding nuclei, as shown in [18]. Thus for light systems, such as  $^{36}\text{Ar}+^{36}\text{KCl}$  or  $^{58}\text{Ni}+^{58}\text{Ni}$ , the bombarding energy required to achieve sufficient initial compression for there to be significant radial expansion is higher than for the heavier systems like  $^{129}\text{Xe}+^{nat}\text{Sn}$  and  $^{197}\text{Au}+^{197}\text{Au}$ . This explains why the  $\Delta$ -scaling transition occurs at higher energy for  $^{58}\text{Ni}+^{58}\text{Ni}$  than for  $^{129}\text{Xe}+^{nat}\text{Sn}$ . For the very light  $^{36}\text{Ar}+^{36}\text{KCl}$  system the threshold is higher still than for  $^{58}\text{Ni}+^{58}\text{Ni}$ , outside the range of measured bombarding energies. On the other hand, for  $^{197}\text{Au}+^{197}\text{Au}$  both the greater initial compression and the far larger Coulomb contribution may come into play in order to reduce the fragment formation time-scale even at the lowest bombarding energy.

We have shown that, for finite systems, the largest cluster size distribution in critical aggregation models is an admixture of the two asymptotic distributions observed far below and above the critical region. This result holds true for both equilibrium (percolation) and out-of-equilibrium (irreversible aggregation) models. A similar decomposition has been shown for the experimentally-observed charge distribution of the largest fragment per event produced in nuclear multifragmentation, indicating that the critical domain lies around  $E_{\text{beam}} \approx 30\text{MeV/A}$  for the  $^{129}\text{Xe}+^{nat}\text{Sn}$  system. By analogy with the irreversible aggregation model, where the form of the order parameter distribution depends on the time-scale of the process, we interpret such criticality along with the corresponding change of  $\Delta$ -scaling as the onset of an “explosive” multifragmentation regime in which initially com-

pressed heated nuclear liquid clusterizes in the presence of significant radial expansion [19]. The mass-dependence of the energy at which the onset occurs for different (symmetric) systems is related to nuclear stopping and hence to transport properties of hot nuclear matter. Such an overall picture is both consistent with, and provides a link between, recent results on the role of radial expansion in nuclear multifragmentation [15, 20] and the systematic study of nuclear stopping around the Fermi energy [18].

The authors would like to thank the staff of the GANIL Accelerator facility for their continued support during the experiments. D. G. gratefully acknowledges the financial support of the Commissariat à l'Énergie Atomique and the Conseil Régional de Basse-Normandie. This work was also supported by the Centre National de la Recherche Scientifique and by the Ministère de l'Éducation Nationale.

---

\* Corresponding author; Electronic address:  
john.frankland@ganil.fr

- [1] B. Borderie and M. Rivet, *Progress in Particle and Nuclear Physics* **61**, 551 (2008).
- [2] R. Botet and M. Płoszajczak, *Physical Review E* **62**, 1825 (2000).
- [3] R. Botet and M. Płoszajczak, *Universal Fluctuations - The Phenomenology of Hadronic Matter* (World Scientific Lecture Notes in Physics, 2002).
- [4] R. Botet, M. Płoszajczak, A. Chbihi, B. Borderie, D. Durand, and J. Frankland, *Physical Review Letters* **86**, 3514 (2001).
- [5] J. D. Frankland, A. Chbihi, A. Mignon, M. L. B. Blaich, R. Bittiger, B. Borderie, R. Bougault, J. L. Charvet, D. Cussol, R. Dayras, et al., *Physical Review C* **71**, 034607 (2005).
- [6] E. J. Gumbel, *Statistics of Extremes* (Columbia University Press, New York, 1958).
- [7] J. Pouthas, B. Borderie, R. Dayras, E. Plagnol, M. Rivet, F. Saint-Laurent, J. Steckmeyer, G. Auger, C. Bacri, S. Barbey, et al., *Nuclear Instruments and Methods in Physics Research Section A: Accelerators, Spectrometers, Detectors and Associated Equipment* **357**, 418 (1995).
- [8] P. G. J. van Dongen and M. H. Ernst, *Physical Review Letters* **54**, 1396 (1985).
- [9] B. Zheng and S. Trimper, *Physical Review Letters* **87**, 188901 (2001).
- [10] R. Botet, *The Seventh Workshop on Particle Correlations and Femtoscopy* (University of Tokyo, Japan, 2011).
- [11] W. Verkerke and D. Kirkby, *RooFit Users Manual v2.91* (2008), URL [ftp://root.cern.ch/root/doc/RooFit\\_Users\\_Manual\\_2.91-33.pdf](ftp://root.cern.ch/root/doc/RooFit_Users_Manual_2.91-33.pdf)
- [12] D. Stauffer and A. Aharony, *Introduction to Percolation Theory* (Taylor & Francis Publishers, London, 1994).
- [13] W. Bauer, *Phys. Rev. C* **38**, 1297 (1988).
- [14] X. Campi, H. Krivine, N. Sator, and E. Plagnol, *Eur. Phys. J. D* **11**, 233 (2000).
- [15] E. Bonnet, B. Borderie, N. Le Neindre, M. Rivet, R. Bougault, A. Chbihi, R. Dayras, J. Frankland, E. Galichet, and F. Gagnon-Moisan, *Nuclear Physics A* **816**, 1 (2009).
- [16] E. Plagnol, J. Lukasik, G. Auger, Ch. N. Bellaize, F. Bocage, B. Borderie, R. Bougault, R. Brou, P. Buchet, et al., *Physical Review C* **61**, 014606 (1999).
- [17] L. B. Yang, E. Norbeck, W. A. Friedman, O. Bjarki, F. D. Ingram, R. A. Lacey, D. J. Magestro, M. L. Miller, A. Nadasen, R. Pak, et al., *Phys. Rev. C* **60**, 041602 (1999).
- [18] G. Lehaut, D. Durand, O. Lopez, E. Vient, A. Chbihi, J. D. Frankland, E. Bonnet, B. Borderie, R. Bougault, E. Galichet, et al., *Physical Review Letters* **104**, 232701 (2010).
- [19] W. Bauer, J. P. Bondorf, R. Donangelo, R. Elmer, B. Jakobsson, H. Schulz, F. Schussler, and K. Sneppen, *Phys. Rev. C* **47**, R1838 (1993).
- [20] E. Bonnet, B. Borderie, N. Le Neindre, A. Raduta, M. F. Rivet, R. Bougault, A. Chbihi, J. D. Frankland, E. Galichet, F. G. Moisan, et al., *Physical Review Letters* **105**, 142701 (2010).